RENORMALIZATION GROUP METHOD: EFFECTS OF DIFFUSION RETARDING ON INTRACELLULAR MEMBRANES

O. Posnansky*[1], Y. Kupriyanova[1], and N. J. Shah[1,2]
[1]Medical Imaging Physics, Institute of Neurosciences and Medicine - 4, Forschungszentrum Jülich GmbH, 52425 Jülich, Germany, [2]Department of Neurology, Faculty of Medicine, JARA, RWTH Aachen University, Aachen, Germany

1. Introduction: Proton self-diffusion demonstrates superb sensitivity to the biological properties of living tissue. In tissue, an interplay between different compartments and structures presents different amounts of hindrance to diffusing spins. The presence of restricting cellular structures in neural tissue leads to non-Gaussian dynamics of the diffusion-weighted imaging (*DWI*) signal inside a voxel. The microscopic origins of this phenomenon are still not well understood. The restrictions can potentially originate from many sources such as microtubules, neurofilaments, proteins, lipids, and cholesterol. In the present work, retarding effects on axon membranes were included in the renormalization-group (RG) method [1, 2]. Effects of microparameters on diffusivity in neurons were investigated. It was shown that the presence of axon membranes leads to non-Gaussian diffusion.

2. Methods: Following the *Basser-Sen* model [3], we characterize coated fibres by D_m (myelin-sheath diffusion), D_a (axon diffusion) and corresponding proton densities c_a, c_m, which have outer (R_m) and inner (R_a) radii. Axon diffusivity is restricted by flat, infinitely thin membranes. These membranes are randomly oriented and embedded in the axons in a way depicted in Fig.1. We hypothesize that membranes exhibit delay (or retarding) effects in water molecule propagation. Due to this phenomenon axon diffusion can be depicted by equivalent circuit scheme with complex-valued impedance and frequency ω [4]. Eq.1 describes "classical" retarding effects, where $D_{mem} = d\,k\,l$ (here, k, is membrane permeability, l, its thickness and, d, is topological dimension), i is an imaginary unit, and τ is a characteristic retarding time. Fibres with membrane substructure and complex-valued diffusivity are immersed in an extra-cellular space, the Wigner-Seitz (*WS*) cell, with diffusion D_e, proton density c_e and linear size L (Fig.2). We calculate the diffusive properties of *WS* cell using the *Basser-Sen* model for the case when *WS* is occupied with a fibre and the empty *WS* cell is assigned with extra-cellular properties. Two types of *WS* cells can be randomly distributed on the square lattice with probability p that *WS* cell is empty and $(1-p)$ that *WS* is occupied with fibre (Fig.2, a black *WS* cell indicates fibre occupation).On the square lattice with randomly occupied cells it is possible to outline the *2x2 RG* block. All non-degenerative configurations of black and white *WS* cells on the scale *2x2* of *RG* block are presented in Fig.3. In Fig.4 the process of scale renormalization is depicted for the specific distribution of *WS* cells. Mathematically, such an *RG* process can be described by a system of nonlinear equations (Eq.2, n is an iteration step number). Details on construction of the system Eq.2 can be found in [1,2].

3. Results: Initial parameters estimating macroscopical dynamic diffusive properties of heterogeneous brain white matter are listed in Table1. The transversal diffusivity $D_t(\omega) = \lim_{n\to\infty} D_t^n(\omega)$ and its normalized value $D_t^{norm}(\omega) = \left(D_t(\omega) - D_e\right)/\left(D_e \cdot (1-p)\right)$ were calculated according iterative scheme described by Eq.2. The real and imaginary parts of $D_t^{norm}(\omega)$ calculated for $p \in [0;1]$ and $\tau = 1$ are shown in Fig.5a,b. The yellow cross-line gives diffusion at the most interesting biologically relevant limit $p = 0.2$. The real and imaginary parts of $D_t^{norm}(\omega)$ for fixed $p = 0.2$ and various $\tau = \{0.1;0.3;0.9;1\}$ noted on corresponding curves are shown in Fig.6a,b. It is clear that two bounds are valid for time-dependent $D_t(t) = F^{-1}\left(D_t(\omega\tau)\right) = \left\{\approx D_e\big|_{\omega\tau>>1}; D_a\big|_{\omega\tau<<1}\right\}$ [4]; here symbol F^{-1} means inverse Fourier-transform operator.

Results for the effective apparent diffusion coefficient $ADC_{eff}(t)$ (Eq.3) were obtained in the case of short-time limit, $t << \tau$, where supposed b-value $\sim t$ in $\ln(S/S_0) = -ADC_{eff}\,b$ and longitudinal diffusivity D_l was calculated according *Basser-Sen* scheme. The extracellular volume fraction was $p = 0.2$. We observed three regimes of behaviour of the diffusion-weighted signal (Fig.7, thick black curve). Zones I and III present pure Gaussian regimes characterized with upper, $\omega\tau >> 1$, and lower, $\omega\tau << 1$, bounds of retarding times. Zone III presents Gaussian asymptotic due to "homogenization" of strongly heterogeneous neuronal structure in large time of diffusion scale. Zone II exhibits "switching" between two Gaussian limits and defined by spectrum of retarding times. The broadness of the spectrum determines the extent of non-Gaussian diffusion profile and *kurtosis* of curve in separating zone II. Various tangent curves (thin dashed lines shifted to the origin of coordinate system) with responses $\tau = \{0.1;0.3;0.9;1\}$ noted in Fig.7. Clear that on time scales $\tau_{I,\min} \le \tau < \tau_{I,\max}$ and $\tau_{III,\min} \le \tau < \tau_{III,\max}$ retarding responses are singular, and on scale $\tau_{II,\min} \le \tau < \tau_{II,\max}$ retarding effects exhibit dispersion properties.

4. Discussion and Conclusions: We analyzed nonlinear behaviour of time dependent diffusivity on the cellular level of the tissue and provided an explanation of the non-Gaussian diffusion profile as a function of the membrane retarding times. Measurement of either $ADC_{eff}(\omega)$, or the $ADC_{eff}(t)$, is suggested as a means to experimentally determine cell membrane retardation of diffusivity from the *DWI* signal. Correlating retarding effects with tissue physiology may lead to novel contrast between healthy and diseased tissues. Such a contrast could be especially revealing in stroke for which membrane changes may play a key role.

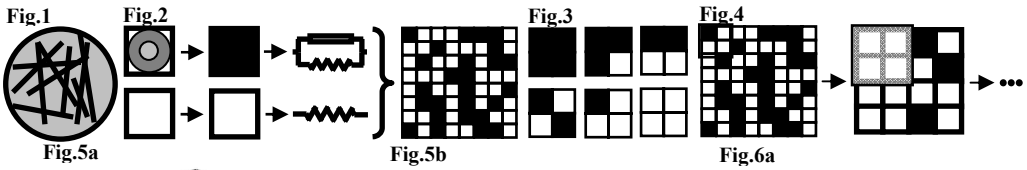

Table 1

Parameter X	*Input value*	R_a	$6.57*10^{-6}\,m.$
p	[0;1]	R_m	$4*10^{-6}\,m$
D_e	$2*10^{-9}\,m^2/s$	c_e	.95
D_m	$.3*10^{-9}\,m^2/s$	c_m	0.5
D_{mem}	$.75*10^{-9}\,m^2/s$	c_a	0.88

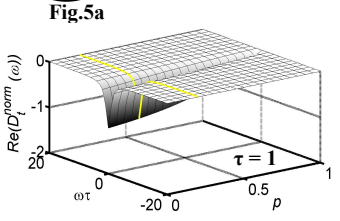

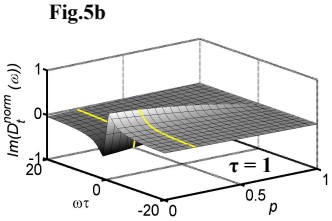

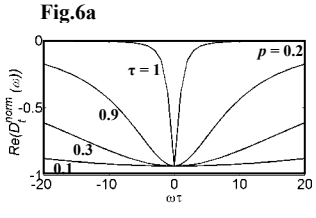

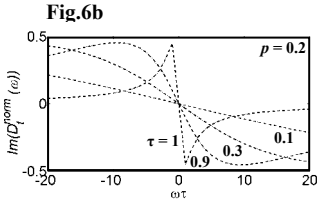

Fig.7

$$\begin{cases} p_{n+1} = \sum_k g_k r_n^k & (2a) \\ P_{n+1} = (1-p_n)\,\delta\left(D_t - D_t^{L,n}\right) + p_n\,\delta\left(D_t - D_t^{U,n}\right) & (2b) \\ D_t^{U,n+1} = \left\langle D_t^{U,n} \right\rangle & (2c) \\ D_t^{L,n+1} = \left\langle D_t^{L,n} \right\rangle & (2d) \end{cases}$$

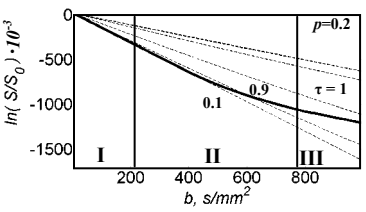

$$D_{a,eff}(\omega) = D_e + \frac{D_{mem} - D_e}{1 + i\omega\tau} \qquad (1)$$

$$ADC_{eff} = \left(2D_t + D_l\right)/3 \qquad (3)$$

5. References: [1] Posnansky O., Shah N., *ISMRM* 2009, 136 [2] Posnansky O., Shah N., J.Biol.Phys.34 (2008), 551. [3] Se P., Basser P., Biophys.J. 80 (2005), 2927. [4] Cole K., Scienc 79 (1934), 164. [*] Current address: Deutsches Diabet Zentrum, 40225 Düsseldorf, Germany.